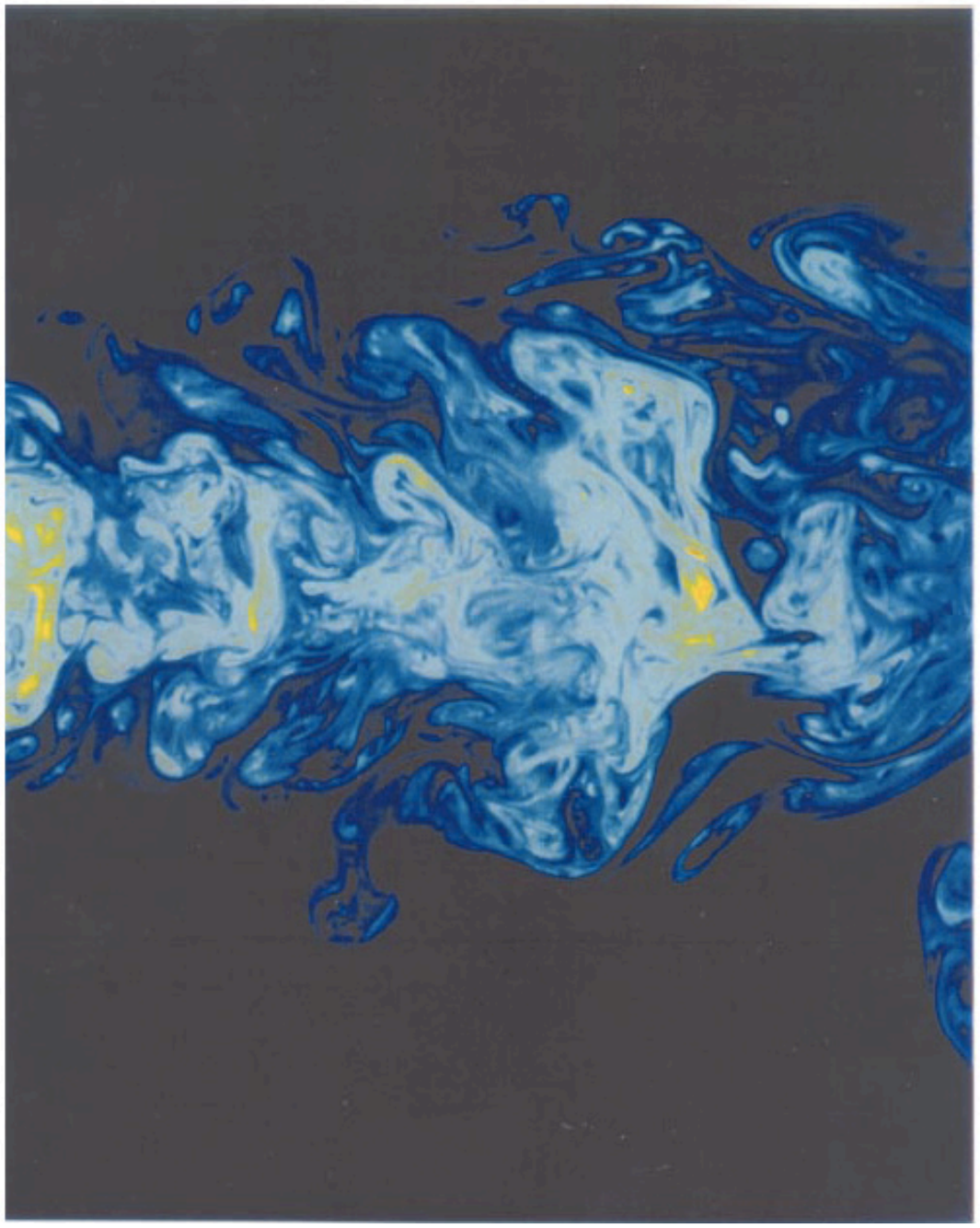

Fractal contours of scalar in a 2D smooth random flow

Marija Vucelja

Gregory Falkovich
Konstantin S. Turitsyn

Courant Institute of Mathematical Sciences,
Weizmann Institute of Sciences,
MIT

Fluorescent dye in a turbulent jet
of Reynolds number Re = 4000
(K. Sreenivasan, 1991)

"Mathematics of particles and Flows" May 2012, WPI

Mixing and transport

- The basic understanding of turbulent mixing and transport:

Taylor, Richardson, Kolmogorov, Obukhov and Corrsin...

from dimensional arguments: **the average rate of spreading** or mixing of e.g. a smoke plume.

- The **statistics of the large fluctuations** is a more difficult problem. The practical relevance:
  - the probability of a pollutant concentration exceeding some tolerable level as it spreads from a source.
  - the role of large concentration fluctuations in controlling the rate of slow (high order) chemical reactions (e.g. in the process of atmospheric ozone destruction).

Zero modes

multipoint correlation functions of scalar and gradient:

Schraiman, Siggia, Chertkov, Falkovich, Kolokolov, Lebedev, Gawedzki, Bernard, Kupiainen

(1994-2000)

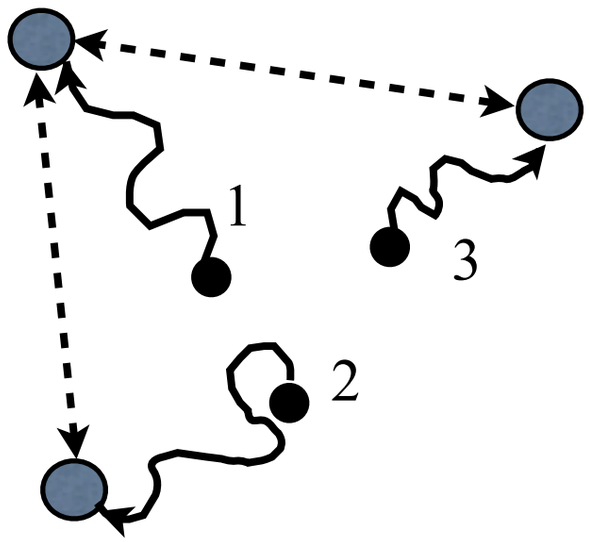

Geometry of points that started close by...

$$\frac{\mathrm{d}\theta}{\mathrm{d}t} = \frac{\partial\theta}{\partial t} + (\boldsymbol{v}\cdot\boldsymbol{\nabla})\theta = \varphi$$

$$\theta(\boldsymbol{R}(t),t) = \int_{-\infty}^{t} \varphi(\boldsymbol{R}(t'),t')\,\mathrm{d}t' \qquad \dot{\boldsymbol{R}}(t) = \boldsymbol{v}(\boldsymbol{R}(t),t)$$

$$\langle\theta(\boldsymbol{r}_1,t)\ldots\theta(\boldsymbol{r}_N,t)\rangle = \int_{-\infty}^{t} \langle\varphi(\boldsymbol{R}(t'_1),t'_1)\ldots\varphi(\boldsymbol{R}(t'_1),t'_N)\rangle\,\mathrm{d}t'_1\ldots\,\mathrm{d}t'_N$$

Passive scalar evolution

We studied a passive scalar under the action of pumping, diffusion, advection in smooth 2D flow with Lagrangian chaos.

$$\partial_t \theta(t, \boldsymbol{r}) + (\boldsymbol{v}(t, \boldsymbol{r}) \cdot \boldsymbol{\nabla}) \theta(t, \boldsymbol{r}) = \kappa_d \boldsymbol{\nabla}^2 \theta(t, \boldsymbol{r}) + \varphi(t, \boldsymbol{r})$$

pumping $\varphi(t, \boldsymbol{r})$

Poisson process of independently adding size-L blobs of passive scalar at random positions and with random amplitudes

L pumping scale

diffusion

κ_d molecular diffusion coefficient

Smooth 2d flow field

Batchelor regime *Batchelor 1959*

Kraichnan model *Kraichnan 1968*

The velocity field: random, smooth and incompressible white in time and of spatially linear velocity profile

$$\sigma_{ij} = \frac{\partial v_i}{\partial r_j}$$

tensor of the local (Lagrangian) velocity gradients

$$\langle \sigma_{ij}(t)\sigma_{kl}(t')\rangle = \lambda[3\delta_{ik}\delta_{jl} - \delta_{ij}\delta_{kl} - \delta_{il}\delta_{jk}]\delta(t-t')$$

λ Lyapunov exponent

Batchelor regime

$$\boldsymbol{v}(t, \boldsymbol{R}_1(t)) - \boldsymbol{v}(\boldsymbol{R}_2(t)) = \sigma(t, \boldsymbol{R}_2(t))(\boldsymbol{R}_1(t) - \boldsymbol{R}_2(t))$$

valid when $|\boldsymbol{R}_1(t) - \boldsymbol{R}_2(t)| < \eta$

$\eta \equiv (\nu^3/\epsilon)^{1/4}$ Kolmogorov (viscous) scale

ν kinematic viscosity

ϵ energy dissipation

$\mathrm{Pr} \equiv \nu/\kappa_d \gg 1$ Prandtl number

Spatial scales

L pumping scale

$r_d \equiv \sqrt{\kappa_d/\lambda}$ diffusion scale

Scalar blob evolution

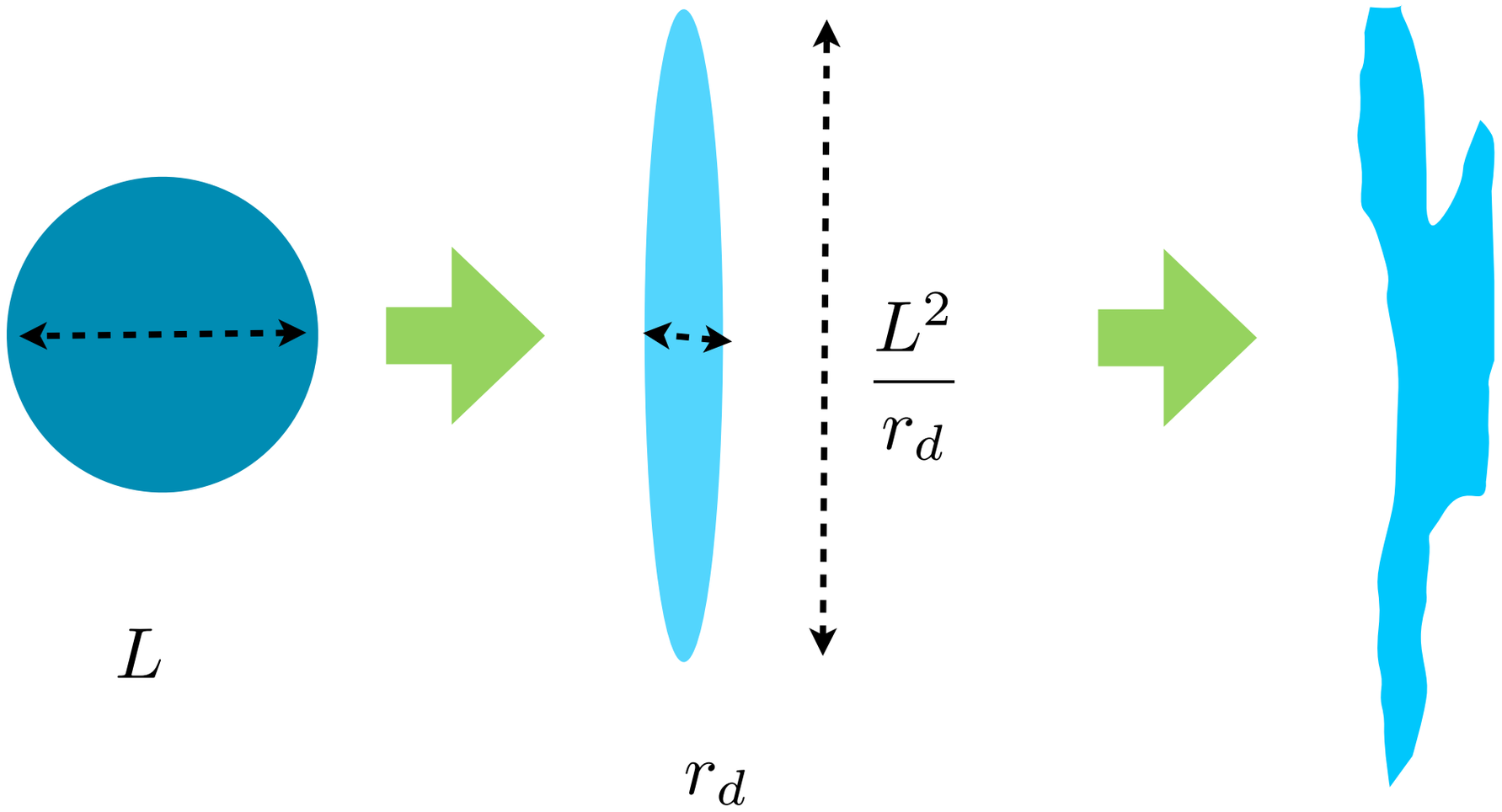

Velocity

Forcing

Smooth flows - a simplest example of mixing

- large-scale mixing in the Earth atmosphere where the turbulence spectrum k^{-3} (the velocity gradients are then well-defined and the flow can be locally considered smooth).
- flows in the phase space of dynamical systems.

Mixing in smooth flows is provided by exponential separation of trajectories and Lagrangian chaos. We consider an incompressible fluid flows which correspond to Hamiltonian flows in phase space.

NEW computational method

- exploiting the linearity of the reaction diffusion equation
- method of characteristic to solve for a single spherical blob of scalar

initial form of blob $\theta(t_0, \boldsymbol{r}_0) = \Theta_0 \exp[-(\boldsymbol{r}_0 - \boldsymbol{r}_c)^2/(2L^2)]$

at a later time

$$\theta(t, \boldsymbol{r}_0) = \frac{\Theta_0 L^2}{\sqrt{\det I(t, t_0)}} e^{-\frac{1}{2}(\boldsymbol{r}(t) - \boldsymbol{r}_c) I^{-1}(t, t_0)(\boldsymbol{r}(t) - \boldsymbol{r}_c)}$$

$\boldsymbol{r}(t) \equiv W(t)\boldsymbol{r}(t_0)$ defines evolution operator $W(t)$

moment of inertia

$$I(t, t_0) \equiv \left(WW^T\right)(t) + \kappa_d \int_0^t \mathrm{d}t' W(t) W(t')^{-1} [W(t) W^{-1}(t')]^T$$

Semi-analytic method allows HUGE resolutions

$$\theta(t, \boldsymbol{r}_0) = \frac{\Theta_0 L^2}{\sqrt{\det I(t, t_0)}} e^{-\frac{1}{2}(\boldsymbol{r}(t)-\boldsymbol{r}_c) I^{-1}(t,t_0)(\boldsymbol{r}(t)-\boldsymbol{r}_c)}$$

seven values specify a blob at time *t*: $I_{11}, I_{12}, I_{21}, \Theta_0, \boldsymbol{r}_c, t_0$

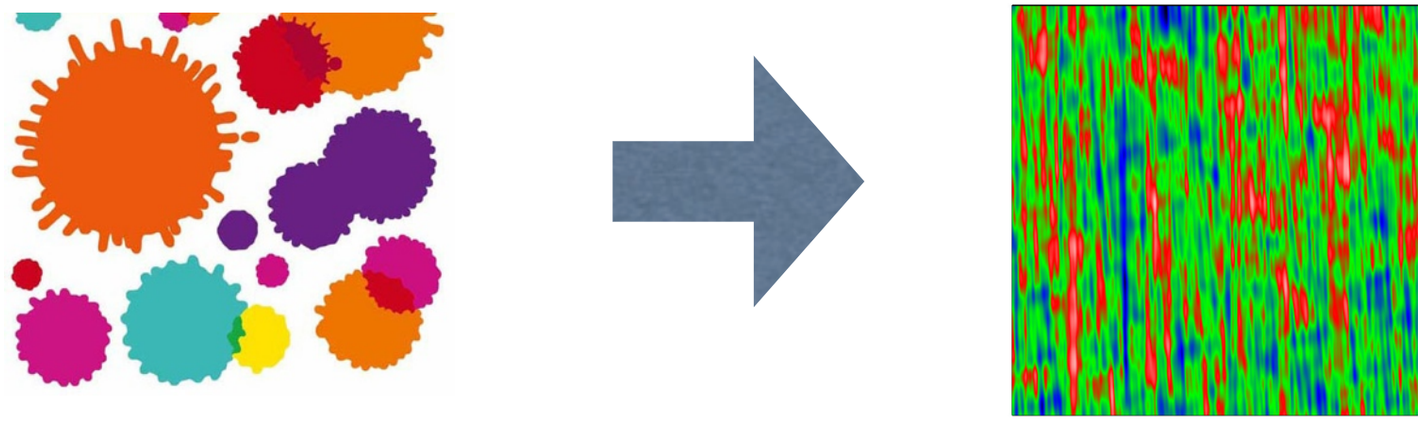

Summing over the blobs can get passive scalar field. Large enough number of blobs assures the Gaussianity of pumping statistics.

Conventional methods out used are pseudospectral and thus always one is limited by the slow decay (logarithmic) of the passive scalar pair correlation function.

A long iso-contour

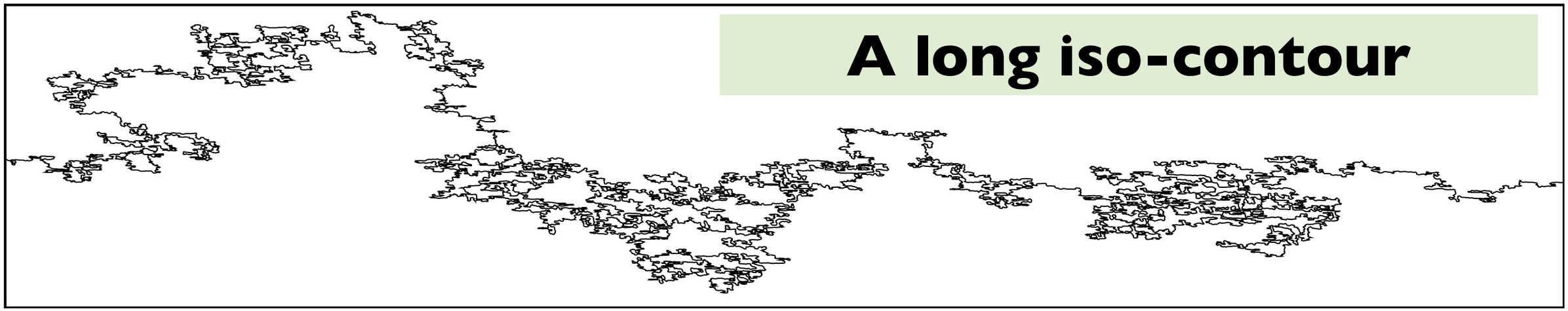

top: 2400 L x 360 L (L pumping scale)
bottom: zoomed inset

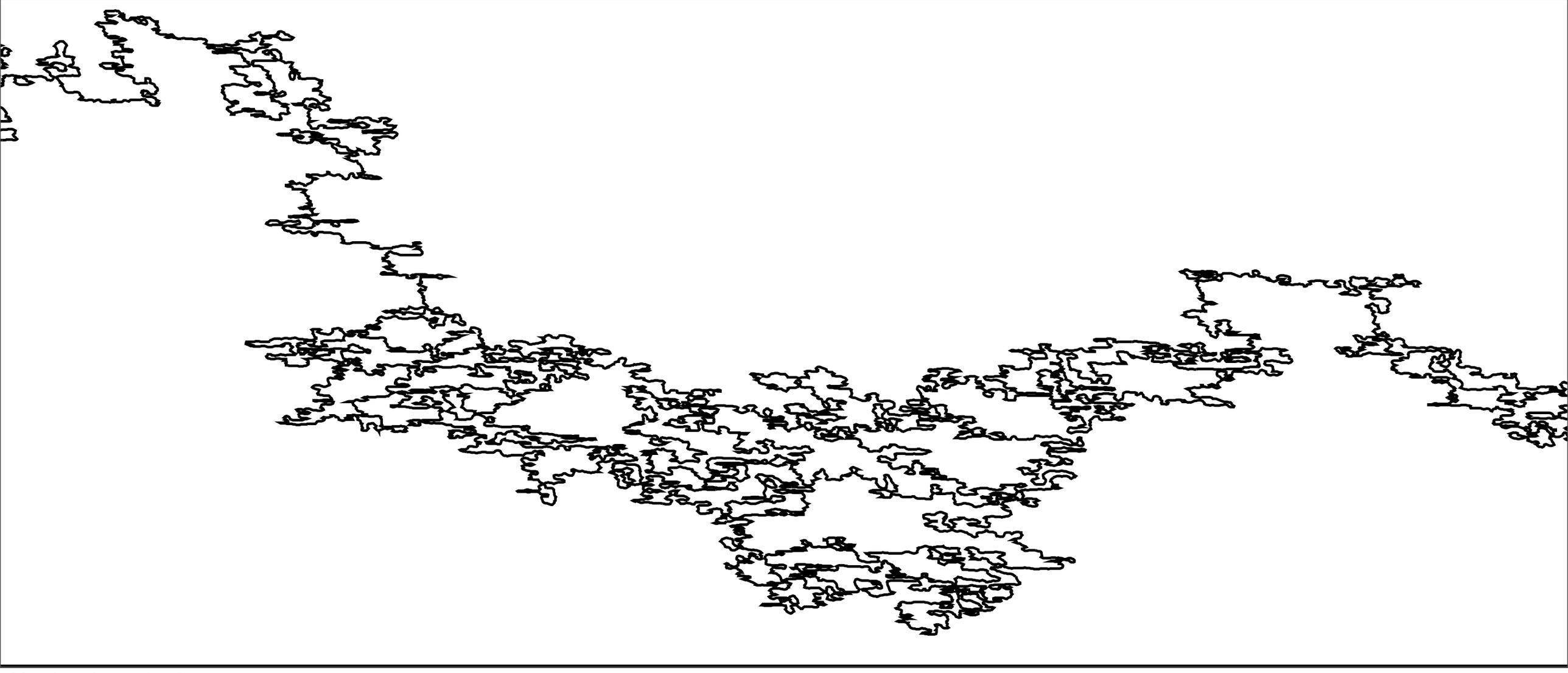

Appearance of fjords of isolines of scalar

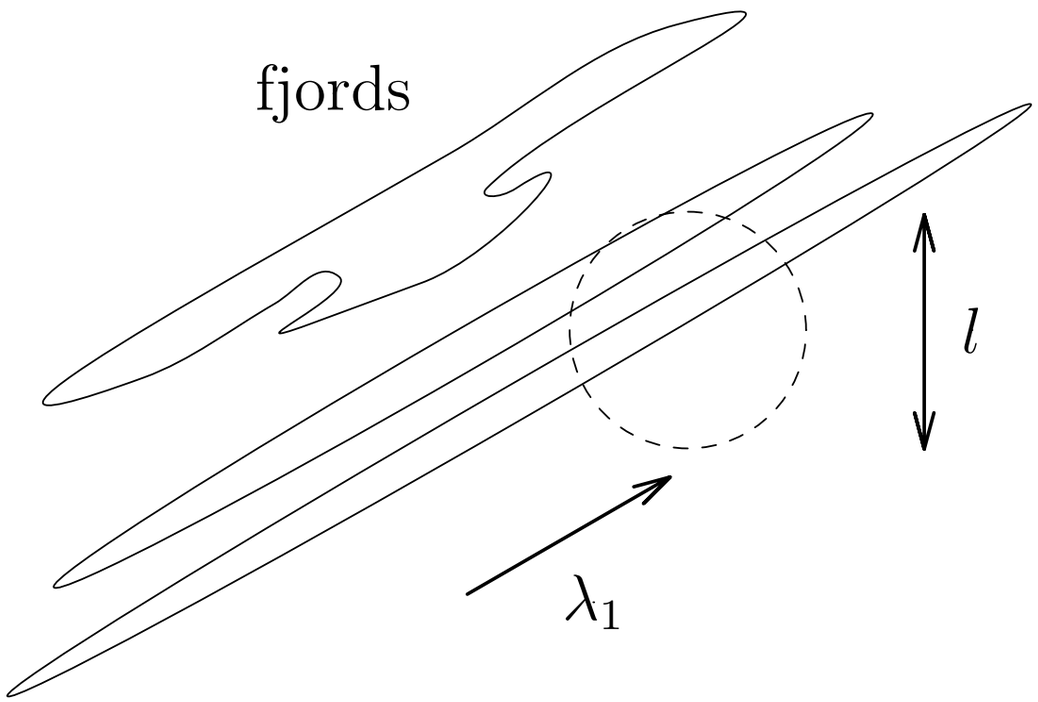

L

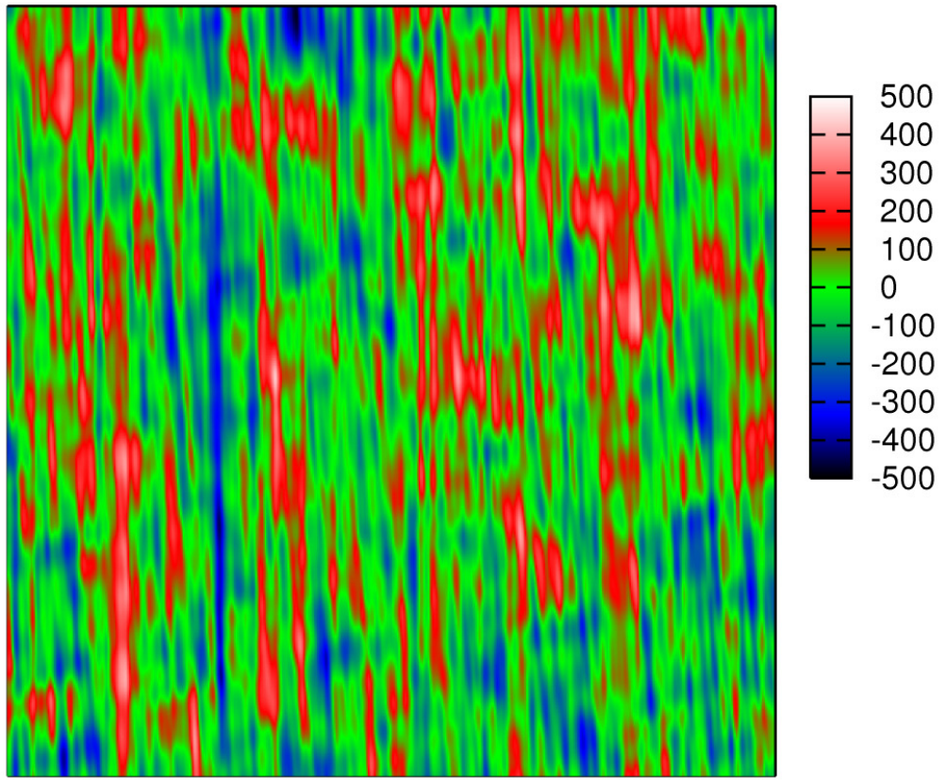

snapshot scalar field 75 L x 75 L

creation of fjords

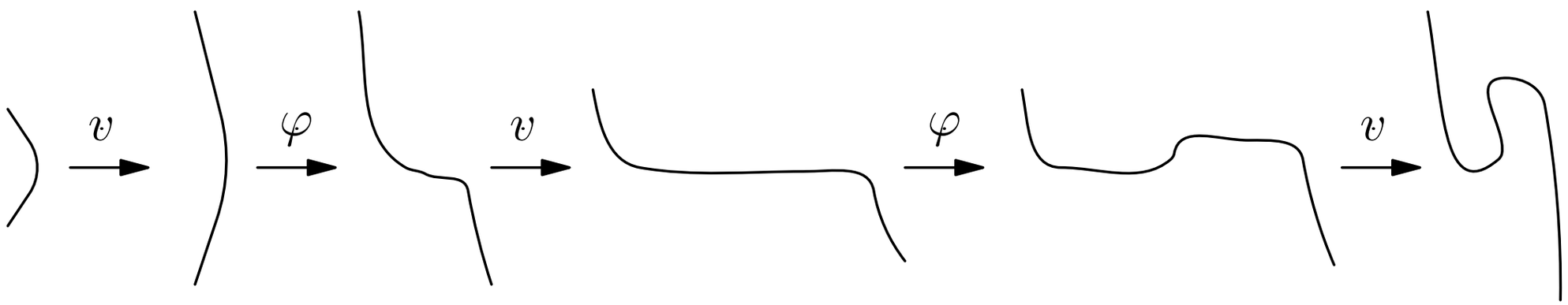

IMPORTANT: diffusion randomly reconnects the curves

Statistics of nodal lines

Expectations - "trivial statistics"

- pumping alone would produce a Gaussian field θ whose zero isolines are smooth at the scales below *L*, while at larger scales they are equivalent to critical percolation (SLE_6 , $D_0 = 7/4$).

- $\boldsymbol{v}$ does not change the statistics of θ as it just rearranges it; the flow stretches isolines uniformly at the direction of and contracts them λ_1 transversal to it.

Actually: Non-trivial statistics

Non-trivial statistics and its isolines arises from an interplay of velocity, pumping and finite diffusivity or finite resolution, which leads to the dissipation of scalar and reconnection of isolines that came closer than the resolution scale.

Non-gaussian field

$$\mathcal{P}\{\theta\} \propto \exp\left[-\frac{\mu}{2}\int \mathrm{d}\boldsymbol{r}|\boldsymbol{\nabla}\theta(\boldsymbol{r})|^2/\chi(\boldsymbol{0})\right],$$

$$\frac{\partial \mathcal{P}}{\partial t} = \frac{1}{2}\iint \mathrm{d}\boldsymbol{r}_1\,\mathrm{d}\boldsymbol{r}_2 \frac{\delta^2}{\delta\theta(\boldsymbol{r}_1)\delta\theta(\boldsymbol{r}_2)}\left[K_{\alpha\beta}\nabla_\alpha\theta(\boldsymbol{r}_1)\nabla_\beta\theta(\boldsymbol{r}_2)\right.$$
$$\left.-\chi(\boldsymbol{r}_1-\boldsymbol{r}_2)\right]\mathcal{P} + \kappa_d\int \mathrm{d}\boldsymbol{r}_1 \frac{\delta}{\delta\theta(\boldsymbol{r}_1)}\Delta\theta(\boldsymbol{r}_1)\mathcal{P}.$$

substituting PDF in FP equation first term

$$\iint \mathrm{d}\boldsymbol{r}_1\,\mathrm{d}\boldsymbol{r}_2 D\mathcal{P}\{2[\boldsymbol{\nabla}\theta(\boldsymbol{r}_1)\cdot\boldsymbol{\nabla}\theta(\boldsymbol{r}_2)]^2$$
$$-|\boldsymbol{\nabla}\theta(\boldsymbol{r}_1)|^2|\boldsymbol{\nabla}\theta(\boldsymbol{r}_2)|^2\}.$$

Indeed we know that correlation functions include cumulants.
Our scalar is a non-gaussian field...

No conformal invariance

$F_4 = \langle \theta_1 \theta_2 \theta_3 \theta_4 \rangle$ four point correlation function

Conformal symmetry restricts a four point correlation function:

$$F_4 = f\left(\frac{r_{12}r_{34}}{r_{13}r_{24}}, \frac{r_{12}r_{34}}{r_{14}r_{23}}\right)(r_{12}r_{34}r_{14}r_{23}r_{13}r_{24})^a$$

For passive scalar we know that

$$F_4 = F(\boldsymbol{r}_{12}, \boldsymbol{r}_{34}) + F(\boldsymbol{r}_{13}, \boldsymbol{r}_{24}) + F(\boldsymbol{r}_{14}, \boldsymbol{r}_{23})$$

Balkovsky et al 1995

NOTE: this is not Wick theorem!

BOTH equations satisfied by

$$F(x,y) = (xy)^{a/2} + (xy^{-2})^{a/2} + (x^{-2}y)^{a/2}$$

$$F_4 = (r_{12}r_{34})^{2a} + (r_{13}r_{24})^{2a} + (r_{14}r_{23})^{2a}$$

i.e. to a Gaussian statistics, which is not the case, as we have just shown. Passive scalar is not in any way close to a free field and its statistics is not conformally invariant.

PDF of contour perimeters

P - perimeter

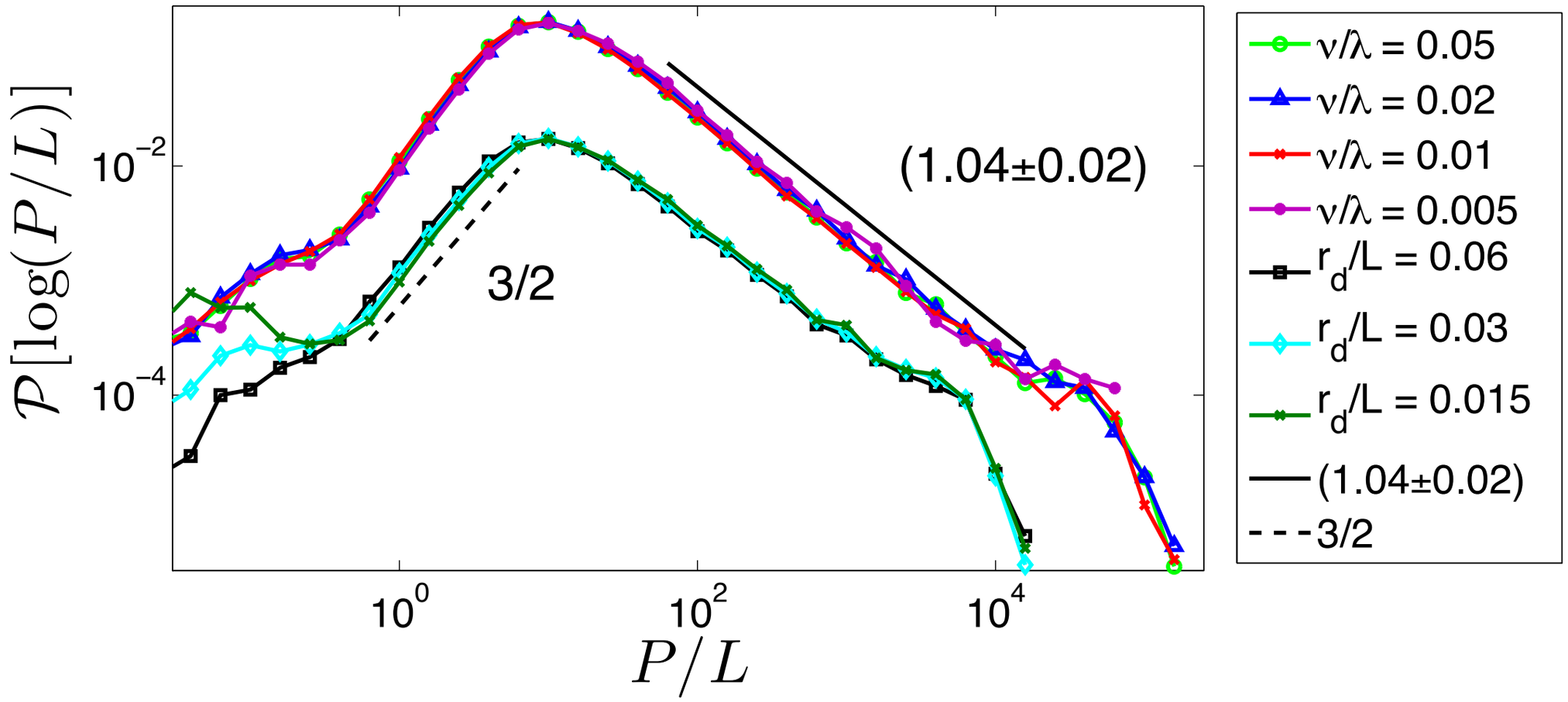

ν/λ pumping frequency

r_d/L resolution

All collapse on top of one another (lower three curves shifted down by dividing by 10)

PDF of sizes (mean radius R)

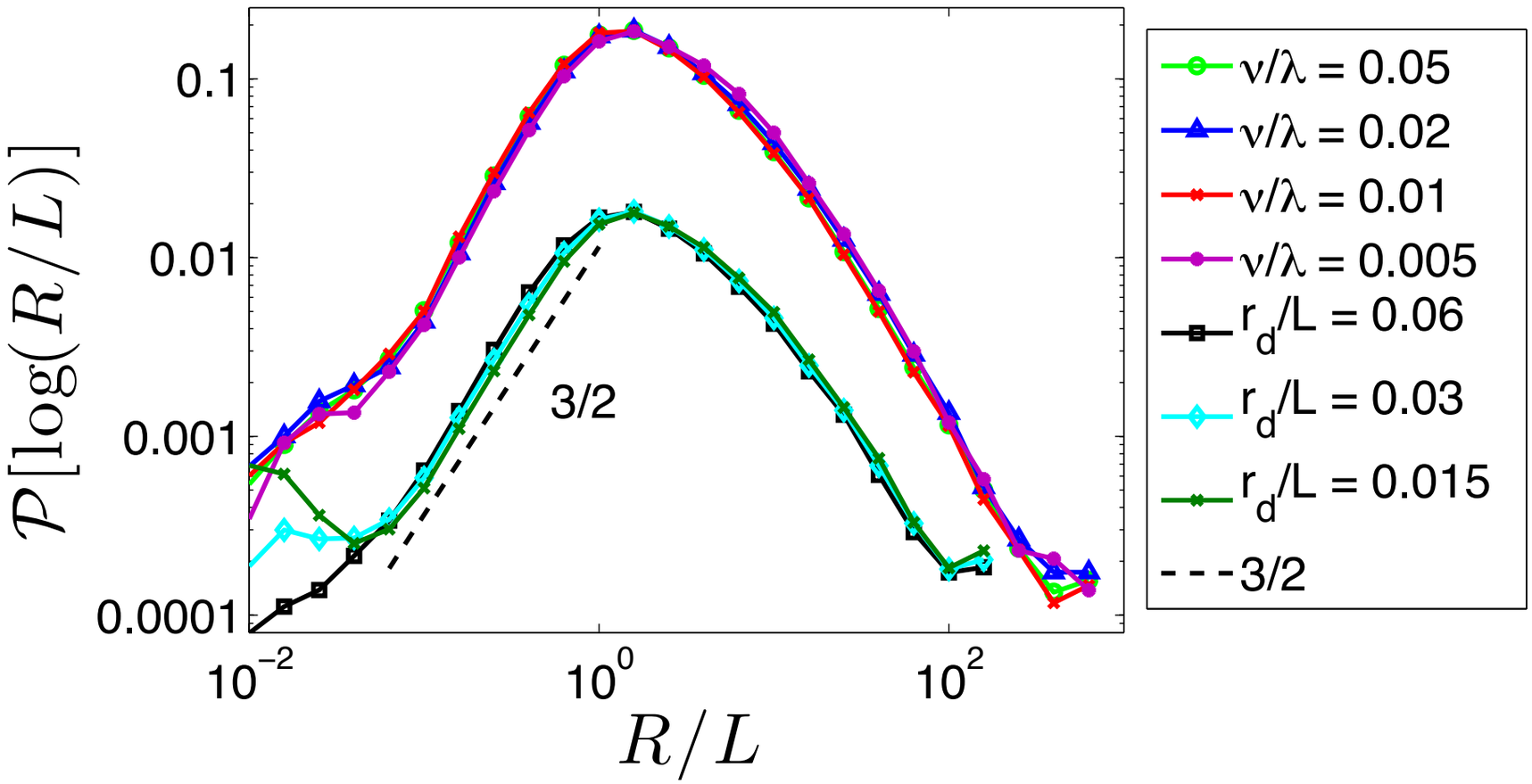

$$R \equiv \sqrt{\langle (\boldsymbol{\rho} - \langle \boldsymbol{\rho} \rangle)^2 \rangle}$$

All collapse on top of one another (lower three curves shifted down by dividing by 10)

Salient features of PDFs of P and R

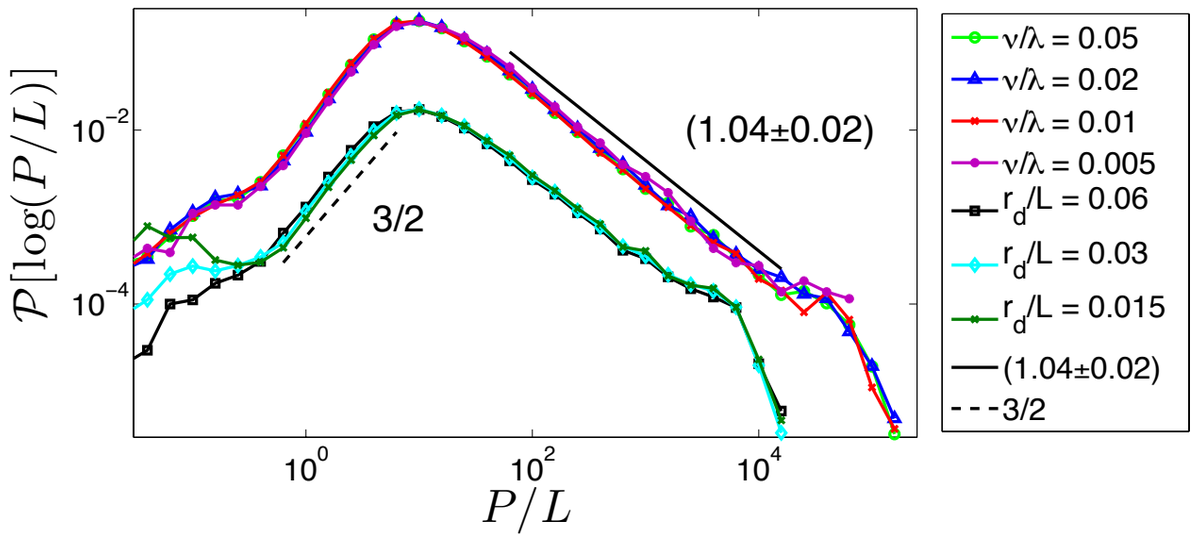

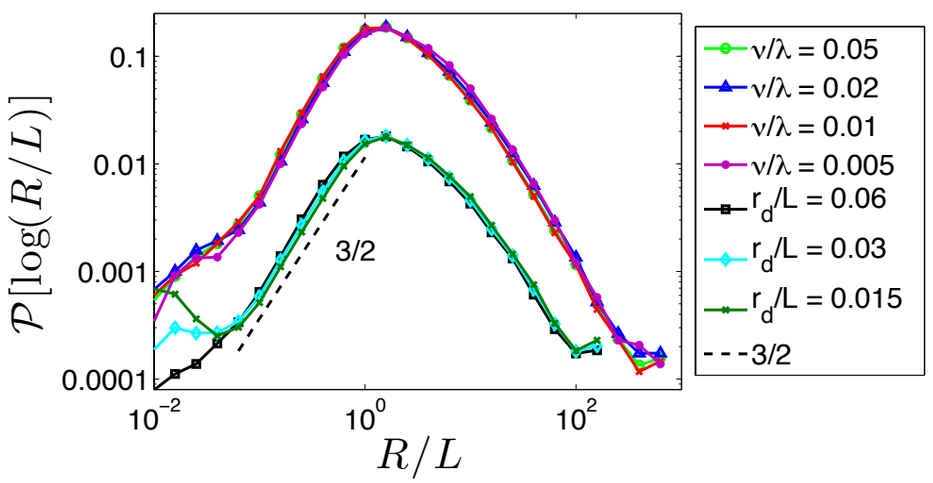

Left tails: 3/2. Contours shorter than L must appear when pumping cuts a piece off a thin long contour, the probability of such a cut is $P \propto R$. Extra factor $\sqrt{P} \propto \sqrt{R}$ in the PDF may appear because to be observed small contours need to survive without being swallowed by further pumping events. Since creation and survival are independent events, their probabilities are multiplied.

Right tail PDF of P: In log coordinates the tail is close to P^{-1}

$$\mathcal{P}(P) \propto P^{-2}$$ *(no theoretical explanation so far)*

generalized box counting fractal dimension

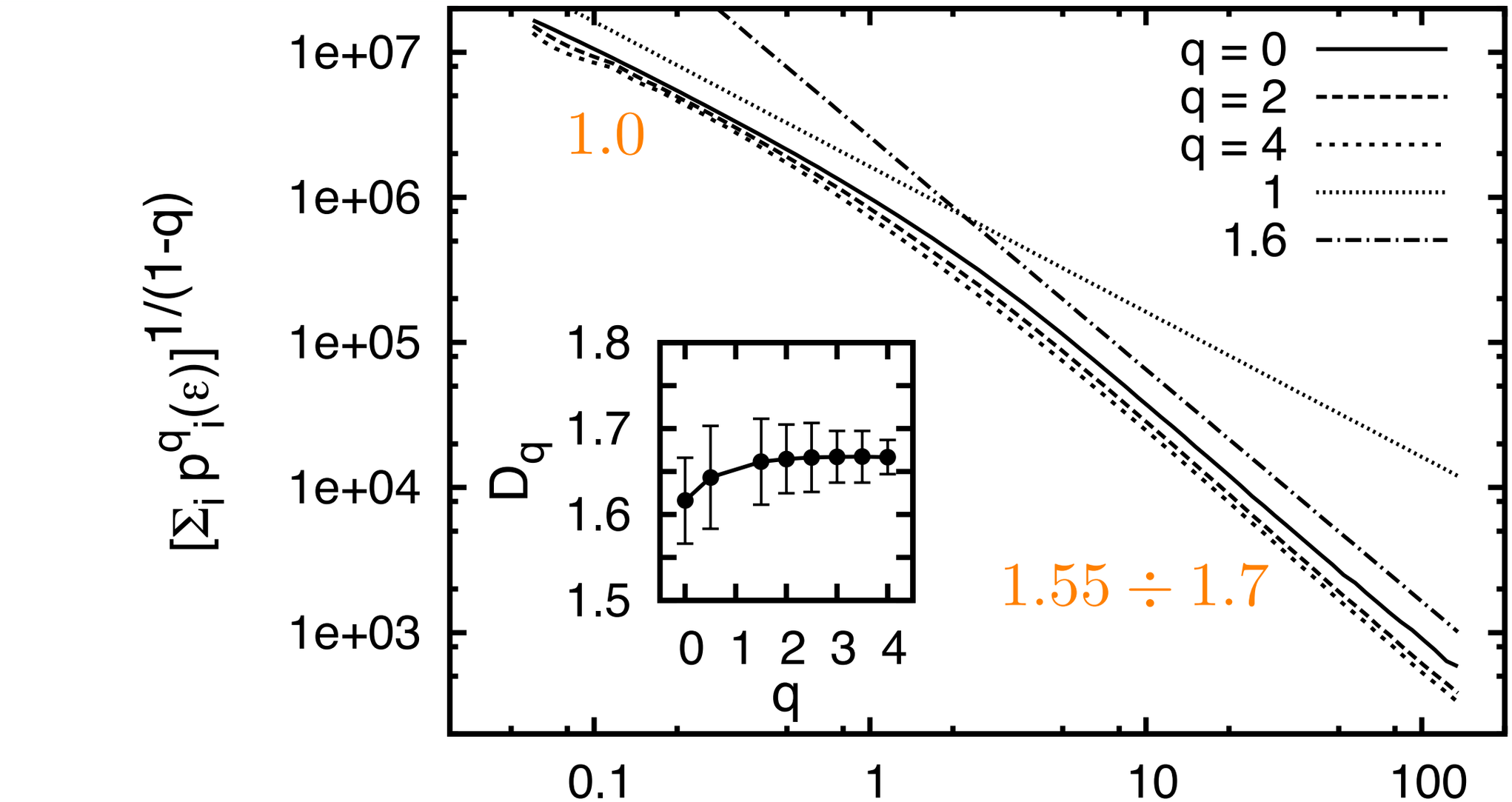

fractal dimension is scale dependent

$$D_q \equiv \lim_{\varepsilon \to 0} \log \left(\sum_i^{N(\varepsilon)} p_i^q(\varepsilon) \right) \left[(q-1) \log(\varepsilon) \right]^{-1}$$

box counting fractal dimension

$1.55 \div 1.7$

1.0

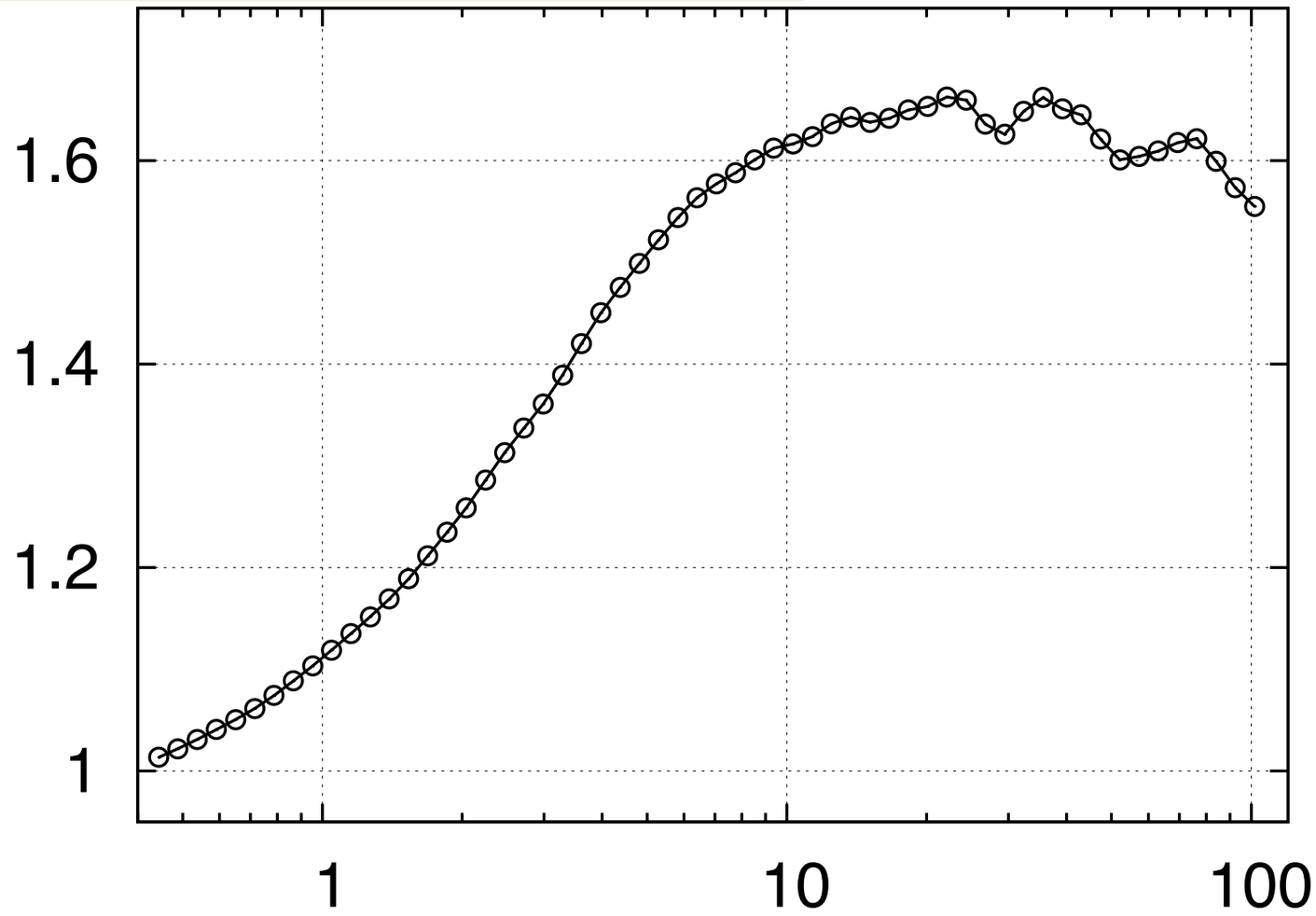

box counting fractal dimension $D_0 = \lim_{\epsilon \to 0} \frac{\ln(N(\epsilon))}{\ln(\epsilon^{-1})}$

estimated from $\mathrm{d}\log N(\varepsilon)/\,\mathrm{d}\log(L/\varepsilon)$

It is scale dependent: bellow forcing scale it is smooth, above it is fractal.

Mono fractals

ν/λ	D_0	D_2	D_4
0.05	1.61 ± 0.05	1.66 ± 0.02	1.67 ± 0.02
0.02	1.62 ± 0.03	1.65 ± 0.05	1.65 ± 0.05
0.01	1.62 ± 0.05	1.67 ± 0.05	1.67 ± 0.03
0.005	1.62 ± 0.03	1.68 ± 0.06	1.68 ± 0.04

Within our accuracy, we cannot see any difference between the dimensionalities of the different orders and conclude that our contours are mono-fractals in distinction from multi-fractal iso-vorticity contours in a direct cascade of $2d$ turbulence This difference might be due to the fact that all parts of our scalar contours go through the same history of velocity, while parts of a long vorticity contour may have different histories.

Characterize curves with SLE
(Schramm-Loewner Evolution)

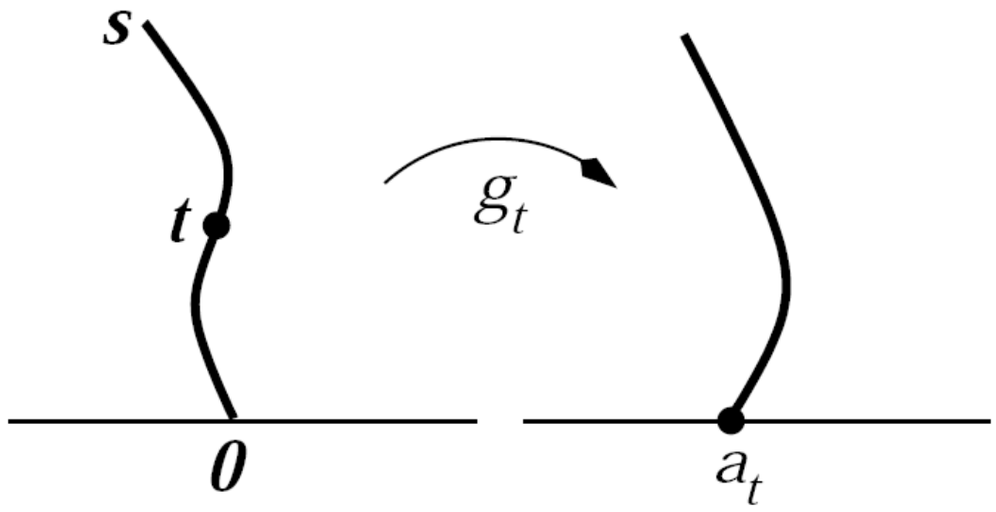

$$\frac{\mathrm{d}g_t(z)}{\mathrm{d}t} = \frac{2}{g_t(z) - a_t}$$

Loewner, 1923
Schramm, 2000

- g_t conformal map with which the tip of the curve is mapped into the real axis

- a_t driving function

- for Markovian successive maps the driving function at is a standard Brownian motion (*Schramm*, 2000): $a_t = \sqrt{\kappa} B_t$

single velocity realization

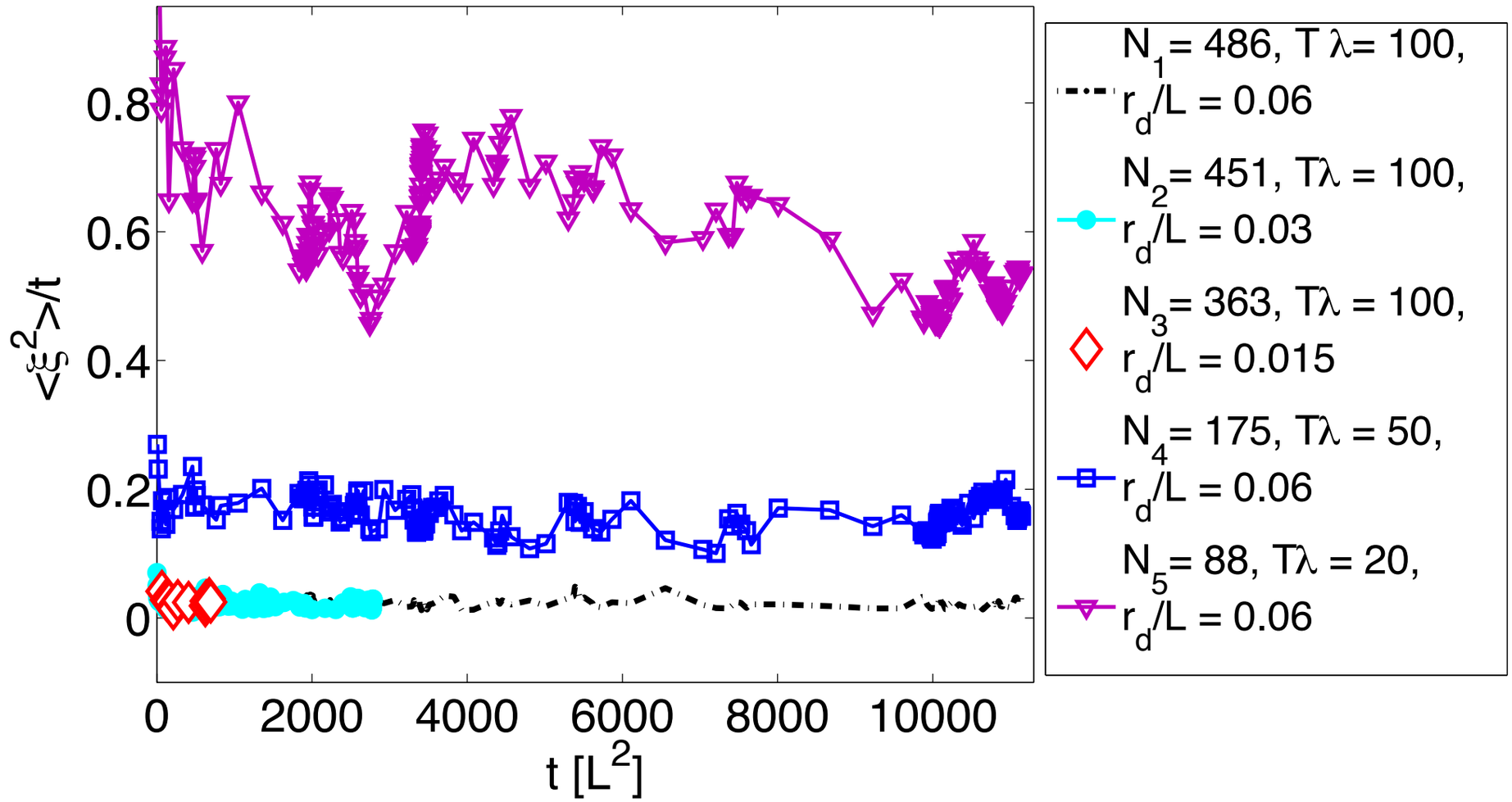

N_i number of contours we averaged over

κ depends on the evolution time, does not depend on the resolution

The curves of different resolutions are of different length since the time of the Loewner map is measured in the units of length squared and for a better resolution we used a smaller physical window.

Effective diffusivity for different velocity realizations

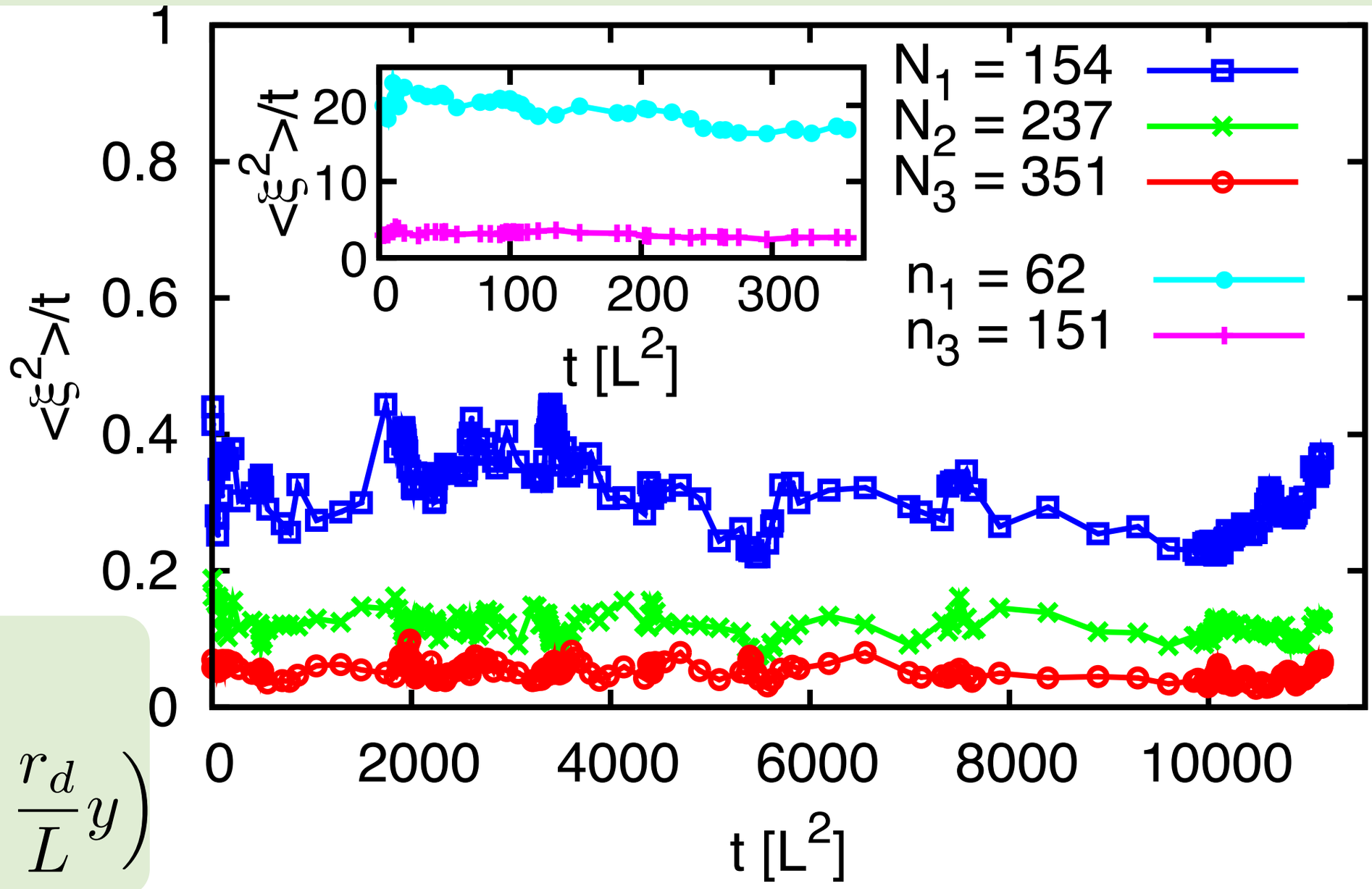

inset

$$(x, y) \to \left(x, \frac{r_d}{L} y\right)$$

Fig. 7 Effective diffusivity of the driving function $\xi(t)$ for velocity realizations $(1 \div 3)$, where t is time in Löwner's eq. The curves are ensemble averages of N_i contours (inset: of n_i contours) from the $i-$th velocity realization. Inset shows the effective diffusivity for velocity realizations 1 and 3 after contraction by L/r_d.

Surprises

Statistics of bending of long isolines

- If there was only pumping then the scalar would be a short-correlated field on scales $r > L$ (such as percolation).

- Without diffusion and with infinite resolution, velocity only distorts the field. *The distorted field is not SLE (Kennedy, 2008), still the driving functions tells us a lot about the geometrical properties of bending.*

SLE in experiments: *While the restoration procedure itself may be not very practical since real flows consist of many such domains oriented randomly, the very possibility of it means potential availability of very useful exact formulae describing the statistics of contours.*

Summarizing

- The distribution of contours over sizes and perimeters is shown to depend neither on the flow realization nor on the resolution (diffusion) scale r_d

- The scalar isolines are found fractal/smooth at the scales larger/smaller than the pumping scale.

- **Driving function of the Loewner map:** Behaves like diffusion with diffusivity independent of the resolution yet, most surprisingly, dependent on the velocity realization and the time - beyond the time on which the statistics of the scalar is stabilized: $\lambda^{-1} \ln\left(\frac{L}{r_d}\right)$

our simulations $T_s\lambda \leq 4$ our runs $T_s\lambda \in \{20, 50, 100\}$

Future ideas

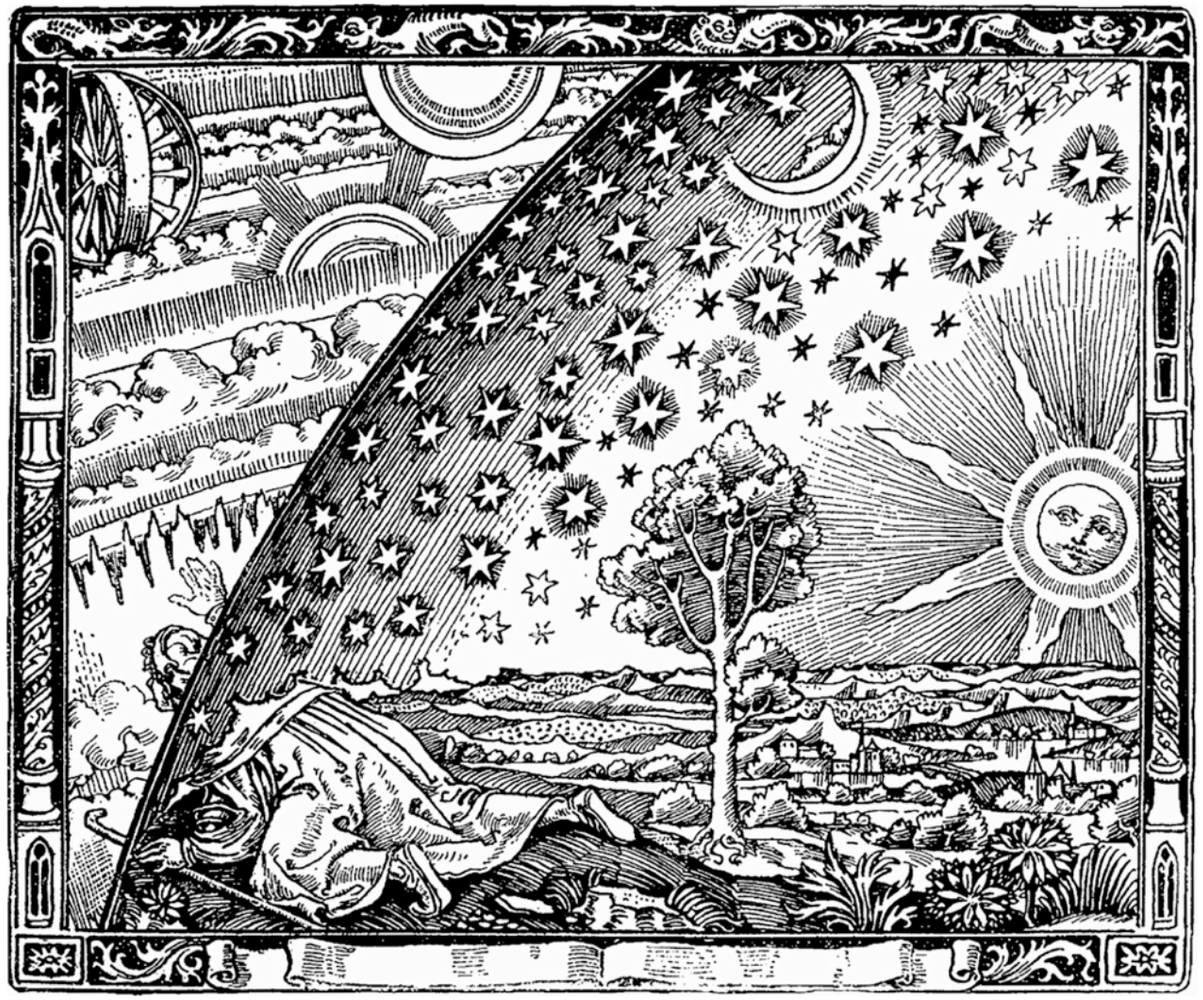

- explain velocity realization dependence of diffusivity
- investigate in detail non-stationarity for isolines?
- other simple models in stochastic geometry